Electrical Engineering in Japan, Vol. 117, No. 4, 1996
Translated from Denki Gakkai Ronbunshi, Vol. 115-D, No. 9, September 1995, 1123-1130

Reduction Control of Induction Motor Vibration with Pulsating Load by Repetitive Control Using an Acceleration Sensor

SHINICHI HIGUCHI, MUNEAKI ISHIDA and TAKAMASA HORI
Mie University

SUMMARY

Recently, the V/F control drive system of the induction motor has been applied widely to the drive of compressors, pumps, etc., because it is very simple and basically requires no speed sensors. However, if the V/F controlled induction motor drives a pulsating load such as the compressors, the rotational speed of the motors is fluctuated considerably and the motor frame vibrates due to the pulsating load torque. When frequency of the torque pulsation is especially close to the resonant frequency of the mechanical system, large vibration and acoustic noise are produced.

In this paper the authors propose a method to reduce the vibration of the V/F controlled induction motor with a fluctuated load by repetitive control using an acceleration sensor. The acceleration sensor is easy to install on the motor or load frame. The repetitive control is considered effective for reduction of the vibration, as the load torque varies periodically. Effectiveness of the proposed method is confirmed by approximate analysis and experiments.

Key words: Induction motor; pulsating load; repetitive control; vibration suppression control; acceleration sensor.

1. Introduction

Induction motors and brushless dc motors are used widely as variable-speed motors because their structure is simple, they are inexpensive, require no maintenance and can be operated in poor environments. In recent years, efficiency considerations have dictated the use of mainly small brushless dc motors [1]. However, large induction motors are utilized widely.

With respect to the speed control schemes of induction motors, they can be divided roughly into speed closed-loop control and speed open-loop control. In the former, there are vector control and slip frequency control. In particular, in the vector control, a high performance similar to a dc machine can be realized. On the other hand, in the latter, there is the V/F-constant control. The features of the V/F-constant control are that speed sensors are not required, and the control system can be implemented simply. Thus, they are used as simple speed control in the drive of compressors of air conditioners, pumps, blowers, etc.

However, when the V/F-controlled induction motor drives a pulsating load such as the compressor of an air conditioner at a low frequency, the rotational speed will fluctuate and the operation becomes unstable, and sometimes noises and abnormal vibrations will occur. Particularly, in the drive at a low frequency close to the mechanical resonant frequency, the vibration will increase and sometimes result in mechanical breakdown. Therefore, the drive at the low frequency is avoided.

In this paper, to make the operation at the low-speed region possible, we have studied the suppression of the fluctuation and vibration of the rotational speed caused by the pulsating load using a simple torque control based on the V/F control. It has been difficult to suppress the vibration effectively in the ordinary speed feedback control because the V/F-controlled induction motor has a complex transient characteristic [2] and the mechanical system is vibrational. Accordingly, we have shown so far that the vibration can be suppressed indirectly by

ISSN0424-7760/96/0004-0109

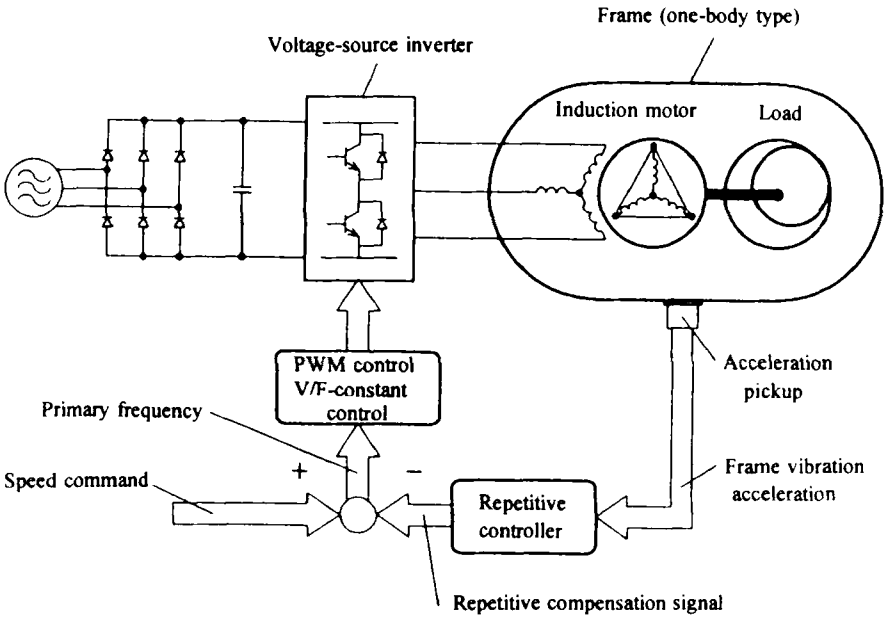

Fig. 1. System configuration.

suppressing the speed variation by means of the repetitive control using speed sensors and the feedforward control [3]. However, as in the case of the compressor of an air conditioner, the installation of the speed sensors may be difficult sometimes due to such problems as load structure and durability of speed sensors.

In this paper, from the viewpoint that the vibration of the frame due to the torque pulsation will be suppressed directly, the acceleration sensor will not be connected to the rotating shaft but instead installed at the outer side of the frame (base), and the repetitive control is carried out by using its signal (Fig. 1). The distinctive feature of the proposed method is that the installation of the acceleration sensor is easy.

In this paper, considering the vibration in the direction around the axis, among the various vibrations which occurred due to the drive of the pulsating load, the effectiveness of the proposed method is shown. To do this, we used experimental equipment which can simulate the pulsating torque of the compressor and the vibration around the rotating axis. Moreover, the stability of the control system is studied by approximate analysis and the theoretical results are compared with the experimental ones.

2. Vibration Suppression Control Method

2.1 Vibration due to pulsating load

For a pulsating load such as that of a compressor for an air conditioner, to prevent the vibration which occurs due to the torque pulsation from spreading to the entire equipment, the load and the motor are installed in a one-body frame and the entire frame is supported by antivibration rubber, etc. In such a structure, when the induction motor drives the pulsating load, the rotational speed of the induction motor will be changed by the difference between the generated torque of the induction motor and the load torque. Moreover, as a reaction of the resultant torque added to the rotating axis, the vibration may occur due to the addition to the frame of the pulsating torque around the rotating shaft. For this reason, if the vibration of this frame is detected by an acceleration sensor, it can be expected that the vibration can be suppressed directly. Further, since this vibration is periodic synchronizing with the rotating period of the load, the repetitive control can be applied.

2.2 Principle of vibration suppression control

The rotational speed of the induction motor is determined at the balanced point between the generated torque of the induction motor and the load torque in

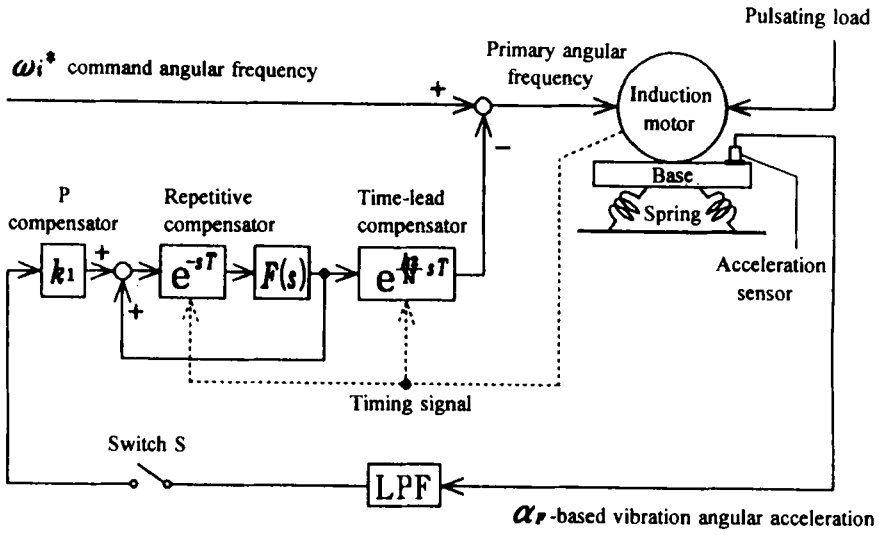

Fig. 2. System block diagram.

steady state. When the load torque changes, the rotational speed will vary by the change and the frame of the inductor motor, and the load will vibrate. Here, to suppress the vibration, it is sufficient to change the generated torque of the induction motor to counterbalance the change of the load torque. To change the torque of the motor, it is sufficient to vary the primary frequency centered around the steady-state operating point.

Figure 2 shows the block diagram of the control system. In this control system, since the induction motor is based on the V/F control, it is a speed open-loop control. The acceleration sensor for detecting the vibration is installed at the common base of the induction motor and load. To execute the repetitive control, it is necessary to detect the period T of the vibration. The timing signal for determining the vibration period may easily be detected by utilizing the operating noise of the compressor valve. Here, in an attempt to verify the principle of the control, a sensor of one pulse per rotation is installed at the motor. Moreover, the Switch S is for stopping the repetitive control in the middle. By using the data obtained at the time point when S is turned off, the vibration suppression control can be carried in an open loop (however, the time signal is required). This will be called the feedforward control here.

In Fig. 2, the constant k_1 is for improving the damping characteristics of the vibration of the repetitive control, the constant k_2 of the time-load compensation is for improvement of the stability of the control system, and $F(s)$ is for improvement of the stability in the high-frequency region. Here, the system becomes a repetitive control system when $F(s) = 1$, and a modified repetitive control system when $F(s) \neq 1$, and the effect of this $F(s)$ will be described later.

2.3 Control algorithm

The outline of the algorithm of the repetitive compensator for performing the experiment is as follows. The repetitive compensator is a compensator which adds the input to the output which is lagging by the vibration period T only if it is described as a continuous system. This algorithm usually is executed by synchronizing with the rotating angle of the rotor. However, since only the timing signal of one pulse per rotation is utilized here, the scheme of dividing the period T into the number of memories only will be used. The repetitive compensator of this scheme can be realized by using a multiplexer, N integrators and a sample holder as shown in Fig. 3. The multiplexer performs the changeover of the input at every interval which is one of N equal divisions of one period based on the previous vibration period T obtained by the timing signal. The input of the repetitive compensator (out of the P compensator) is averaged at every (1/N)T and added to the memory, and afterward its result is held in the memory again.

The output of the repetitive compensator is obtained by reading out the data from the memory immediately before the input is added at every (1/N)T, and holding it

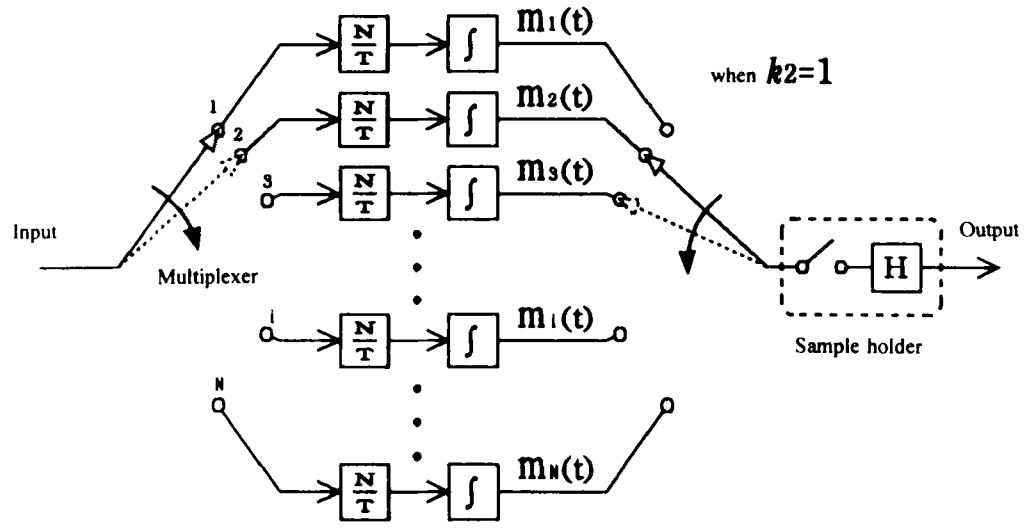

Fig. 3. Structure of the repetitive controller.

during the (1/N)T interval. Moreover, for the time-lead compensator, the time lead of $(k_2/N)T$ can simply be realized by outputting the date of the $(i + k_2)$-th memory immediately before the input is connected to the ith memory. Furthermore, $F(s)$ inside the repetitive compensator can be constructed as a linear phase filter because the repetitive compensator is constructed by the memories.

The proposed method can also cope with the change (i.e., the change of the vibration period T) of the relatively slow rotational speed such as the V/F control.

3. Stability of Repetitive Control System

In the repetitive compensator of Fig. 2, the gain will become infinite for the fundamental component and nth harmonic components of the vibration caused by the torque variations of period T. For this reason, the vibration may diverge (become unstable) depending on the frequency characteristics of the induction motor and compensator. Here, considering the transient characteristics of the induction motor, we study the stability of the system based on perturbation theory and describe a method to determine the feedback constant k_1, constant k_2 of the time-lead compensator and $F(s)$.

3.1 Linear approximation of the system

In the modeling of the system, the inverter is assumed to be an ideal voltage source which will output a sinusoidal voltage, and the coordinate axis (d-axis) is made coinciding with the primary voltage vector. In this case, the voltage equation of the induction motor and the equation of the generated torque can be expressed as follows:

$$\begin{pmatrix} v_{ds} \\ v_{qs} \\ 0 \\ 0 \end{pmatrix} = \begin{pmatrix} r_s+L_sP & -\omega_i L_s & MP \\ \omega_i L_s & r_s+L_sP & \omega_i M \\ MP & -(\omega_i-\omega_r)M & r_r+L_rP \\ (\omega_i-\omega_r)M & MP & (\omega_i-\omega_r)L_r \end{pmatrix} * \begin{pmatrix} -\omega_i M \\ MP \\ -(\omega_i-\omega_r)L_r \\ r_r+L_rP \end{pmatrix} * \begin{pmatrix} i_{ds} \\ i_{qs} \\ i_{dr} \\ i_{qr} \end{pmatrix} \quad (1)$$

$$v_{ds} = \sqrt{2/3}\,\sqrt{2}\,K_{VF}\,\omega_i \ , \ v_{qs} = 0 \quad (2)$$

$$\tau_M = -pM(i_{ds}i_{qr} - i_{qs}i_{dr}) \quad (3)$$

where v_{ds}, v_{qs} are the d-q axis components of the primary voltage space vector; i_{ds}, i_{qs}, i_{dr}, i_{qr} are the d-q axis components of the primary and secondary current space vectors; K_{VF} is the V/F ratio; w_r is the rotor angular velocity referred to frame (electrical angle); w_i is the primary angular frequency; p is the number of pole pairs; and P is the differential operator d/dt.

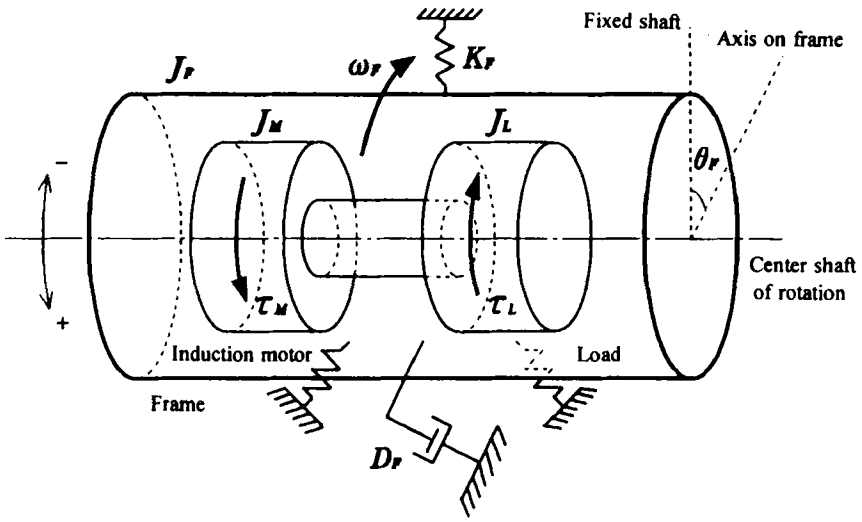

Fig. 4. Model of vibration caused by load torque.

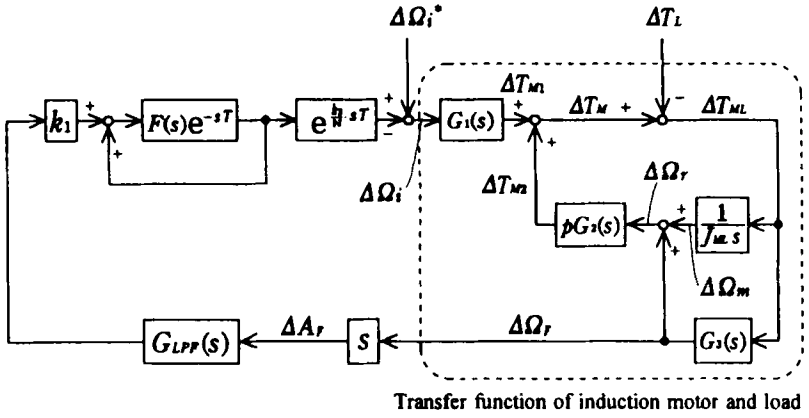

Fig. 5. Block diagram of linearized system.

Moreover, since the difference between the generated torque of the induction motor and the load torque will generate the vibration in the direction around the rotating axis (Fig. 4), the equations of motion of the frame centered around the rotating shaft can be expressed as follows. However, it is assumed that the rotating shaft connecting the rotor of the induction motor and the load has high stiffness and no torsion. Moreover, from the law of action and reaction, the positive direction of θ_F, w_F is opposite to the positive direction of w_r:

$$\tau_{ML} \equiv \tau_M - \tau_L = J_{ML} P \omega_m \tag{4}$$

$$\tau_{ML} = (J_F P^2 + D_F P + K_F)\theta_F \tag{5}$$

$$\omega_F = P\theta_F \ , \ \alpha_F = P\omega_F \tag{6}$$

$$\omega_r = (\omega_m + \omega_F)\frac{p}{} \tag{7}$$

where θ_F is the rotating angle of frame; w_F is the vibration angular velocity of frame; α_F is the vibration angular acceleration of frame; K_F is the spring constant of the vibration-proof rubber (spring) supporting the frame; D_F is the damper coefficient of vibration-proof rubber (spring); J_F is the moment of inertia of the frame; $J_M + J_L$ ($= J_{ML}$) is the moment of inertia of the rotor of induction motor and load; w_m is the rotor angular velocity seen from the fixed base (mechanical angle); and τ_L is the load torque.

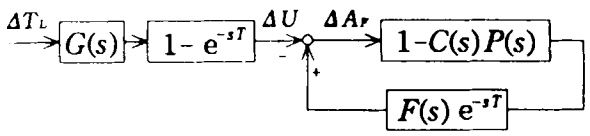

$$C(s)=k_1 \cdot e^{\frac{k_2}{N}sT}$$

$$G_2'(s)=\frac{1}{1-pG_2(s)(1/J_{ML}s+G_3(s))}, \quad G(s)=G_2'(s)G_3(s)s$$

$$P(s)=G_1(s)G_2'(s)G_3(s)G_{LPF}(s)s$$

Fig. 6. Transformed equivalent block diagram.

3.2 Stability of the system

Figure 5 shows the block diagram of the repetitive control system obtained by linear approximation of the equations with respect to displacements around the steady-state operating points. Here, $G_1(s)$, $G_2(s)$ denote the transfer functions of the induction motor; $G_1(s)$ is the transfer function from the primary angular frequency to the torque; and $G_2(s)$ is that from rotating angular velocity to the torque. Moreover, $G_3(s)$ is the transfer function from the torque applied to the frame to the vibration angular velocity, and $G_{LPF}(s)$ is the transfer function of the second-order lowpass filter for noise elimination. Besides, the influence of the averaging process in the input part of the repetitive compensator is neglected here.

Letting w_i^* be constant and paying attention to ΔA_F, the block diagram of Fig. 5 can be rewritten as shown in Fig. 6. Here, if the angular frequency of the torque pulsation is denoted by w_P, since the loop gain of the repetitive control loop will become infinite only in the frequency components of nw_P (n = 1, 2, ...) (when $F(s)$ = 1), it may be considered that the frequency characteristics of $1 - C(s)P(s)$ at the fundamental frequency and the harmonic frequencies nw_P of the torque pulsation will greatly influence the stability of the system and the damping characteristics of the vibration. Moreover, it is assumed that the torque pulsation does not contain the components other than nw_P. Here, when the small gain theorem [4] is applied to the equivalent system of Fig. 5, it is known that the repetitive control system will not diverge from the viewpoint of the input-output stability when

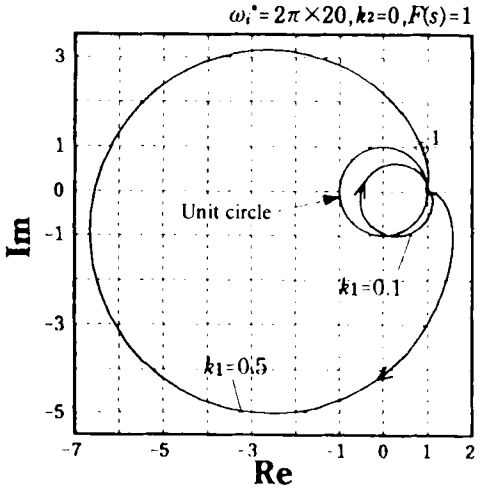

(a) Whole diagram

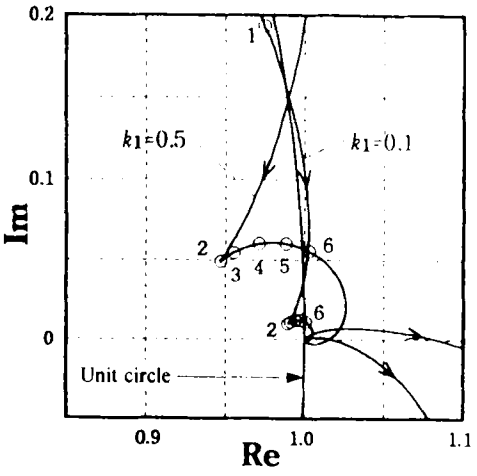

(b) Expanded diagram near 1 + j0

Fig. 7. Nyquist loci of 1 - CP.

$$|1-C(j\omega)P(j\omega)|<\frac{1}{|F(j\omega)|} \quad for \ ^{\forall}\omega \tag{8}$$

However, Eq. (8) is a sufficient condition for stable operation but not a necessary condition. Here, if we pay attention to the frequency of the vibration and its harmonic components, that Eq. (8) holds at $w = nw_P$ (n is a natural number) is a necessary condition. Moreover, in the case of utilizing the repetitive control in order to obtain the data of the feedforward control, it may be sufficient that the temporary convergence of the vibrational components are maintained even if the stability is not strictly guaranteed. Therefore, here, we will study the case of $w = nw_P$.

Table 1. System parameters

Induction motor	Rated output 2.2 [kW]
	Rated voltage 200 [V]
	No. of pole pairs p = 2
	V/F ratio : $K_{VF} = (200/\sqrt{3})/(2\pi \times 60)$
	$l_s = l_r$ = 0.0029 [H], M = 0.0819 [H]
	r_s = 0.86 [Ω], r_r = 0.53 [Ω]
+	$J_{ML} = J_M + J_L$ = 0.076 [kg•m²]
load	J_F = 0.94 [kg•m²]
	D_F = 1.2 [kg•m²•rad/s]
	K_F = 2720 [kg•m²•(rad/s)²]
	Average load torque 2.5 [N•m]
Filter	Cut-off frequency $\omega_c = 2\pi \times 102$ [rad/s]

3.3 Design of compensators

Figure 7 shows an example of the Nyquist loci of $1 - C(jw)P(jw)$. The constants of the test motor are shown in Table 1. The numerals in this figure show the orders of the fundamental and higher harmonic components of the vibration. When the frequency is increased from 0 to ∞, the vector locus will draw the trajectory starting from the point 1 + j0 and returning to 1 + j0. Part of the vector locus is outside the circle. However, the points for the vibrational frequency components must be inside the unit circle. Moreover, when the points inside the unit circle are far from the unit circle, the convergence speed of the vibrational component is faster. By contrast, for the point outside the unit circle, when the distance from the unit circle is farther away, the divergence speed becomes faster.

Here, when the gain k_1 of the compensator is increased, since the vector locus is expanded centered around the point 1 + j0, it is possible to make the convergence speed larger by keeping the points inside the unit circle for the vibrational component farther away from the unit circle. On the other hand, the point outside the unit circle for the vibrational component will become farther away from the unit circle and the divergence speed will also become larger. Moreover, at the mechanical resonant frequency lower than the vibration frequency, the locus also is far outside of the unit circle and may worsen the stability of the system. Therefore, it is desirable to use a small gain k_1 in the range which will not hinder the convergence of the vibration.

However, it is impossible to stabilize the system by the P compensator k_1 alone, and, of course, the vector

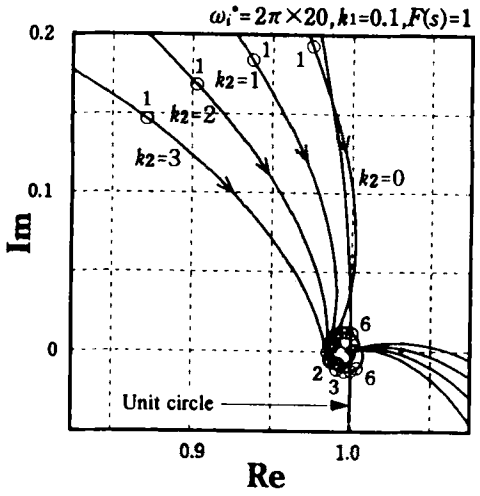

Fig. 8. Nyquist loci of 1 - *CP* (expanded loci).

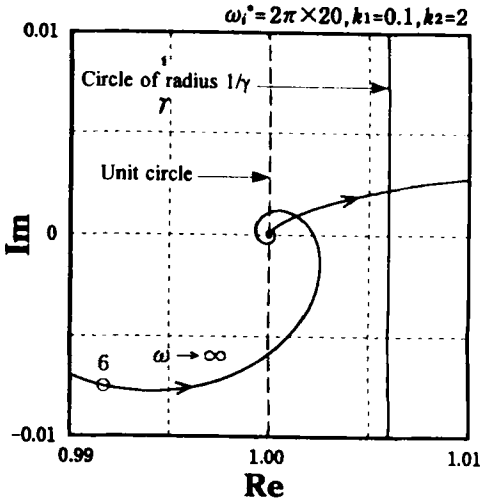

Fig. 9. Nyquist locus of 1 - *CP* (expanded locus).

locus may be found outside the unit circle and be unstable even in the harmonic components, but also in the fundamental wave depending on the command frequency in some cases. As the cause of such a divergence, the phase lag due to the electrical response lag of the induction motor can be considered. Accordingly, it may be possible to keep the fundamental wave and lower-order harmonics inside the unit circle by compensating the phase by employing the lead-time element.

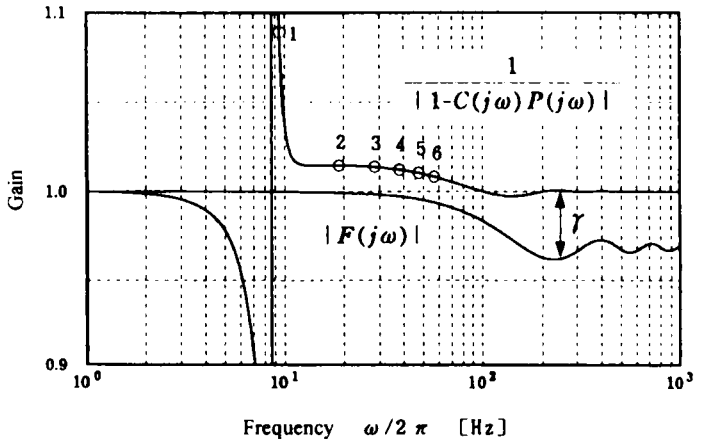

Fig. 10. Relationship between F and 1 - CP.

Table 2. Parameters for experiment of system

Repetitive control	$\omega_i^*=2\pi\times20, k_1=0.1, k_2=1, F(s)=1$
Modified repetitive control	$\omega_i^*=2\pi\times20, k_1=0.1, k_2=2$ $\omega_i^*=2\pi\times30, k_1=0.1, k_2=3$ $f(mt)=\{f((m-1)t)+190f(mt)+f((m+1)t)\}/192$
Control period	T/32 (N=32)

Figure 8 shows the diagram near 1 + j0 when N = 32, k_1 = 0.1 and k_2 is changed from 0 to 3. It is seen that the lower-order harmonic components are inside the unit circle in the case of k_1 = 1 or 2.

However, for the higher-order harmonics, since the vector locus will become spiral counterclockwise centered around the point 1 + j0 (the locus is too small to appear in Fig. 8 when k_2 = 1), the system cannot be stabilized with simple time lead by k_2 alone.

Figure 9 is an expanded diagram near 1 + j0 when k_2 = 0. Here, if we look again at the stability condition based on the small gain theorem of Eq. (9), the stability in the high-frequency region can be improved by making $F(s)$ a lowpass filter. This is due to the fact that since the stable boundary will expand from the unit circle to the circle of radius $1/\gamma$ by the attenuation γ of $|F(jw)|$, the higher-order harmonic components can also easily be kept in the stable region. Here, as shown in Fig. 10, it is sufficient to set $F(s)$ so that it will not intersect $1/\{1 - C(s)P(s)\}$ in the frequency region in question, i.e., the higher-order harmonic frequency. The discrete representation of $F(jw)$ in this case is shown in Table 2. However, to maintain the stability by the attenuation of $F(s)$ means that the frequency band of the vibration suppressor is narrowed and the higher-order harmonic components of the vibration will remain as a steady-state deviation.

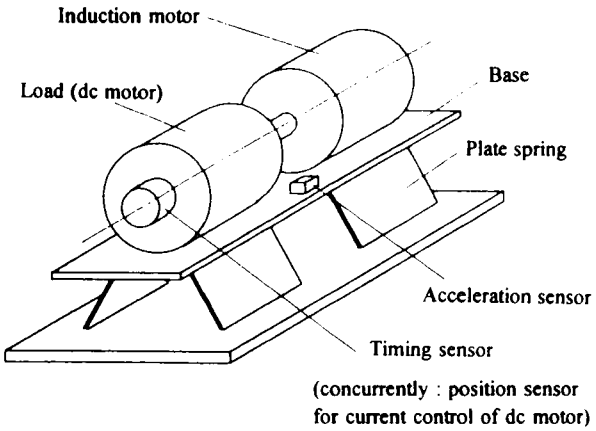

Fig. 11. Mechanical model system for experiment.

4. Experimental Results

4.1 Experimental system

A pulsating-load simulation system is constructed as an experimental system as shown in Fig. 11. In the experimental system, for simulating the vibration of the whole frame of the motor and compressor supported by

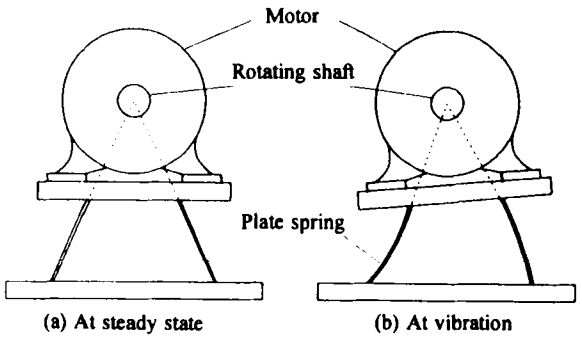

Fig. 12. Vibration around rotating axis.

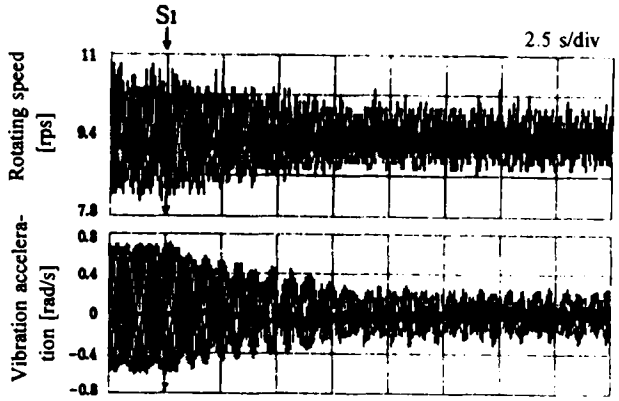

Fig. 13. Reduction of vibration acceleration by modified repetitive control.

the vibration-proof rubber of the air conditioner, the induction motor and the load (dc motor) are installed on a common base (platform) and the base is supported by the plate springs. Here, by installing the plate springs in such a shape that the vibration of the whole frame will occur mainly around the rotating shaft of the rotor (Fig. 12).

Moreover, for simulating the pulsating torque of the compressor of the air conditioner, the current of the load (dc motor) is controlled by a chopper in accordance with the rotating angle of the rotor. Besides, the signal of an encoder of one pulse per revolution installed at the dc motor is utilized for the detection of the period T required in the repetitive control. Furthermore, the control algorithm is executed by a microprocessor MC68000 (control period 500 μs) and the control period of the repetitive compensator is set at T/32 (N = 32).

4.2 Experimental results

The experiment is carried out by using the parameters (Table 2) which guarantee stable operation of the system for the fundamental wave and lower-order harmonic vibration components based on the approximate analysis.

Figure 13 shows the damping processes of the vibration acceleration of the base and the rotational speed variation by repetitive control when the command frequency is fixed at 20 Hz. It can be seen that the vibration acceleration and the speed variation attenuate when the modified repetitive control is started at the timing S_1 in this figure. Moreover, Fig. 14 shows the experimental results when the command frequency is changed after the modified repetitive control is carried out by setting the command frequency at 20 Hz, and changed over to the

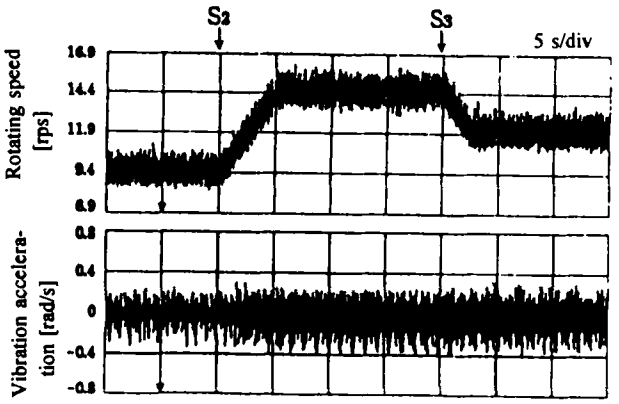

Fig. 14. Vibration acceleration in the case of speed variation by the feedforward control.

feedforward control by turning off S (Fig. 2) at the timing when the vibration attenuated considerably. In this figure, the command frequency is set at 30 Hz at the timing of S_2 and at 25 Hz at S_3. It is seen from the experimental results that the modified repetitive control operates stably even during speed variation.

Figure 15 shows the vibration acceleration of the base and load torque at command frequency 20 Hz. The resonant frequency of the experimental system, determined by the moment of inertia of the frame (induction motor + dc motor + base) and the spring constant of the plate springs is about 8.5 Hz. Since the frequency of the pulsating torque is about 9.5 Hz, which is very close to the resonant frequency, the vibration also occurs primarily. Here, Figs. 16 and 17 show the experimental results by the repetitive control and the modified

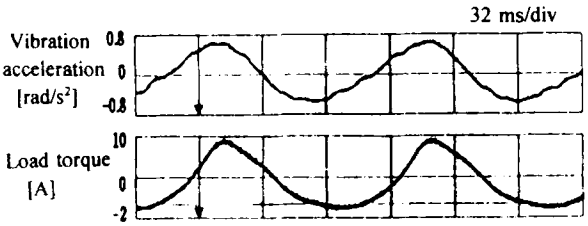

Fig. 15. Experimental result (without the repetitive control).

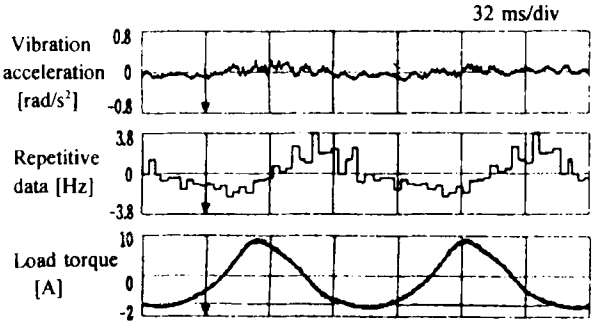

Fig. 16. Experimental result (under the repetitive control).

repetitive control, respectively. It is seen in both results that the fundamental and the lower-order harmonic components of the vibration have been attenuated. However, the higher-order harmonic components remain uncompensated in the case of the repetitive control. Here, it can be confirmed that the repetitive data have diverged by the higher-order harmonic components of the vibration in the repetitive control. By contrast, the divergence by the higher-order harmonic components of the vibration is not seen in the modified repetitive control and the continuous stable control is possible.

Theoretically, the stability in the lower-frequency band cannot be shown. However, as long as the experimental waveforms are observed over an extended period, it is shown that the system is stable. However, in the case where there is uncertainty in stability, it also is possible to change over to the feedforward control by stopping the repetitive control and at the same time setting $F(s) = 1$.

Furthermore, although the experimental data are not shown, it has been confirmed that the system operates stably even for any loads from no load to rated load in

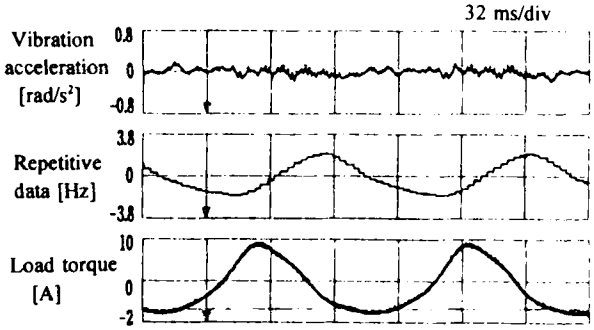

Fig. 17. Experimental result (under the modified repetitive control).

the range of primary frequency 20 to 30 Hz. It has also been confirmed that even over 30 Hz, the damping effect becomes smaller for the vibration of higher harmonics in the modified repetitive control. However, the stability of the system can be maintained.

5. Conclusions

Paying attention to the fact that when an induction motor drives a periodic pulsating load, the vibration which occurs in the frame of the induction motor and its load is a periodic vibration synchronizing with the variation of the load torque. Thus, we have studied the suppression of the vibration by applying the repetitive control and modified repetitive control to the induction motor using an acceleration sensor installed at the frame (base). It has been confirmed by approximate analysis and experiments that the vibration of the frame can be suppressed by the proposed method. The results are summarized below.

(1) An approximate analysis is carried out by small signal linear approximation of the induction motor, and the measures for stabilizing the system are shown for the respective components of the fundamental wave and the higher harmonics of the vibration.

(2) For the fundamental wave and the lower-order harmonic components of the vibration, it is shown that either method of repetitive control or modified repetitive control utilizing the vibration acceleration also is effective.

(3) For the higher-order harmonic components of the vibration, the system becomes unstable in the repetitive control. However, the system becomes stable by

the introduction of the modified repetitive control. The higher-order harmonic components of the vibration cannot be suppressed sufficiently.

(4) For the stability near the resonant frequency of the mechanical system which is lower than the frequency of the vibration, unstable phenomena are not recognized in the experiments. However, the stability cannot be shown theoretically and the modelling method of the system, etc., still remain for study.

(5) It is shown that the vibration suppression is possible if the feedforward control is carried out by using the compensation data obtained by the repetitive control or the modified repetitive control even in the case where the stability of the system cannot be guaranteed with certainty.

Moreover, we have studied in this paper the low-frequency drive. However, we plan to study a method for realizing the vibration suppression control stably over a wider range of speed and load in the future.

REFERENCES

1. Endo, Iizuka and Nakamura. Speed control method of brushless dc motor for vibration suppression of compressor. Documents of the Semiconductor Power Conversion Study Group of the I.E.E., Japan, Vol. SPC-88-63, p. 1, 1988.
2. R. H. Nelson, T. A. Lipo and P. C. Krause. Stability analysis of a symmetrical induction machine. IEEE Trans. on Power Apparatus and Systems, Vol. PAS-88, No. 11, pp. 1710–1717, 1969.
3. Ishida, Ohno and Hori. Suppression control of speed variation of the induction motor with fluctuating load by repetitive learning control. Trans. I.E.E., Japan, Vol. 112-D, No. 1, pp. 12–20, Jan. 1992.
4. Nakano, Inoue, Yamamoto and Hara. Repetitive Control. Society of Instrument and Control Engineers.

APPENDIX

1. Derivation of Transfer Functions $G_1(s)$, $G_2(s)$ of Induction Motor

The induction motor is expressed by linearly approximated transfer functions on the variation of the variables centered around the steady-state operation point.

The primary voltages of the induction motor are, from the V/F-constant control, $w_{ds} = 2/\sqrt{3}\ K_{VF}\ (w_{i0} + \Delta w_i)$, $w_{qs} = 0$. Taking this into account, the variation component of the current, Δi ($i = [\Delta i_{ds}, \Delta i_{qs}, \Delta i_{dr}, \Delta i_{qr}]^T$, will be influenced only by the variation of the primary frequency Δw_i and the variation of the rotational speed Δw_r. Substituting the primary frequency $(w_{i0} + \Delta w_i)$, rotational speed $(w_{r0} + \Delta w_r)$ and current $(i_0 + \Delta i)$ into Eq. (1), neglecting the second-order term of Δ, separating the equations at the steady-state operating point and the variation component, and rearranging, Eqs. (A1) and (A2) can be obtained:

$$\begin{pmatrix} r_s & -\omega_{i0}L_s & 0 & -\omega_{i0}M \\ \omega_{i0}L_s & r_s & \omega_{i0}M & 0 \\ 0 & -S\omega_{i0}M & r_r & -S\omega_{i0}L_r \\ S\omega_{i0}M & 0 & S\omega_{i0}L_r & r_r \end{pmatrix} \begin{pmatrix} i_{ds0} \\ i_{qs0} \\ i_{dr0} \\ i_{qr0} \end{pmatrix} = \begin{pmatrix} 2/\sqrt{3}\ K_{VF}\,\omega_{i0} \\ 0 \\ 0 \\ 0 \end{pmatrix} \tag{A1}$$

$$\begin{pmatrix} r_s+L_sP & -\omega_{i0}L_s & MP & -\omega_{i0}M \\ \omega_{i0}L_s & r_s+L_sP & \omega_{i0}M & MP \\ MP & -S\omega_{i0}M & r_r+L_rP & -S\omega_{i0}L_r \\ S\omega_{i0}M & MP & S\omega_{i0}L_r & r_r+L_rP \end{pmatrix} \begin{pmatrix} \Delta i_{ds} \\ \Delta i_{qs} \\ \Delta i_{dr} \\ \Delta i_{qr} \end{pmatrix} = \begin{pmatrix} L_s i_{qs0}+M i_{qr0}+2/\sqrt{3}\ K_{VF} \\ -L_s i_{ds0}-M i_{dr0} \\ L_r i_{qr0}+M i_{qs0} \\ -L_r i_{dr0}-M i_{ds0} \end{pmatrix} \Delta\omega_i + \begin{pmatrix} 0 \\ 0 \\ -L_r i_{qr0}-M i_{qs0} \\ L_r i_{dr0}+M i_{ds0} \end{pmatrix} \Delta\omega_r \tag{A2}$$

where $S = (w_{i0} - w_{r0})/w_{i0}$.

Similarly, from Eq. (3) of the generated torque, the variation component $\Delta\tau_M$ of the generated torque with respect to the variation component Δi of the current can be obtained as follows:

$$\Delta\tau_M = -pM(i_{ds0}\,\Delta i_{qr} + i_{qr0}\,\Delta i_{ds} - i_{qs0}\,\Delta i_{dr} - i_{dr0}\,\Delta i_{qs}) \tag{A3}$$

From the equation after Laplace transformation of Eq. (A2), the variation component Δi of the current is determined and substituted into Eq. (A3). Moreover, the steady-state value i_0 of the current is determined from Eq. (A1) and substituted into it, and after rearrangement, the following equation can be obtained:

$$\Delta T_M = G_1(s)\,\Delta\Omega_i + G_2(s)\,\Delta\Omega_r \qquad \text{(A4)}$$

where

$$G_1(\lambda\,\omega_{i0}) = \frac{\Delta T_{M1}}{\Delta\Omega_i} = \frac{K}{\omega_{i0}}\,\frac{\beta_{10}\lambda^3+\beta_{11}\lambda^2+\beta_{12}\lambda+\beta_{13}}{\lambda^4+\alpha_0\lambda^3+\alpha_1\lambda^2+\alpha_2\lambda+\alpha_3} \qquad \text{(A5)}$$

$$G_2(\lambda\,\omega_{i0}) = \frac{\Delta T_{M2}}{\Delta\Omega_r} = \frac{K}{\omega_{i0}}\,\frac{\beta_{20}\lambda^3+\beta_{21}\lambda^2+\beta_{22}\lambda+\beta_{23}}{\lambda^4+\alpha_0\lambda^3+\alpha_1\lambda^2+\alpha_2\lambda+\alpha_3} \qquad \text{(A6)}$$

where $\lambda = s/w_{i0}$; and for K, $\alpha_0 \sim \alpha_3$, $\beta_0 \sim \beta_3$, they are as shown in the Appendix table.

2. Derivation of Transfer Function $G_3(s)$ of Vibration Generation Model

The transfer function of the vibration generation model can be obtained from the equations of motion of the frame centered around the rotating axis, Eqs. (5) and (6), as the following equation:

$$G_3(s) = \frac{\Delta\Omega_F}{\Delta T_{ML}} = \frac{s}{J_F s^2 + D_F s + K_F} \qquad \text{(A7)}$$

Table. Coefficients of transfer functions $G_1(s)$, $G_2(s)$

$$\alpha_0 = 2(X_r+X_s)/\sigma$$

$$\alpha_1 = S^2+1+2X_rX_s/\sigma+((X_r+X_s)/\sigma)^2$$

$$\alpha_2 = 2(S^2X_s+X_r)/\sigma+2X_rX_s(X_r+X_s)/\sigma^2$$

$$\alpha_3 = \varepsilon_1/\sigma^2$$

$$\beta_{10} = -SX_s-X_r$$

$$\beta_{11} = \sigma S^2-SX_rX_s-(SX_s+X_r)(X_r+X_s)/\sigma$$

$$\beta_{12} = -S^2X_s(2S-1)-X_r-(2S+1)(X_r+X_s)X_rX_s/\sigma$$

$$\beta_{13} = \sigma S^2+2S^2X_rX_s(1-1/\sigma)-(2S-1)(SX_s)^2/\sigma -(2S+1)(X_rX_s)^2/\sigma-X_r^2/\sigma$$

$$\beta_{20} = X_r$$

$$\beta_{21} = -\sigma S^2+X_rX_s+X_r(X_r+X_s)/\sigma$$

$$\beta_{22} = -2S^2X_s+X_r+X_rX_s(2X_r+X_s)/\sigma$$

$$\beta_{23} = -\sigma S^2-(SX_s)^2/\sigma+X_r^2(X_s^2+1)/\sigma$$

$$K = p(2/\sqrt{3}\,K_{VF})^2(1-1/\sigma)X_r/L_s\varepsilon_1$$

$$X_r = r_r/\omega_{i0}L_r\ ,\quad X_s = r_s/\omega_{i0}L_s\ ,\quad \sigma = 1-M^2/L_sL_r$$

$$\varepsilon_1 = (\sigma^2+X_s^2)S^2-2X_rX_s(\sigma-1)S+(X_s^2+1)X_r^2$$

AUTHORS (from left to right)



Shinichi Higuchi graduated in 1994 from the Department of Electronic Engineering, Mie University. He is currently in the Master's program.

Muneaki Ishida received his Dr. of Eng. degree in 1980 from Nagoya University, where he became a Research Associate in the Department of Electrical Engineering. He has been an Associate Professor in the Department of Electrical Engineering, Mie University, since June 1987. He received a Paper Award from the I.E.E., Japan in 1993. He is a member of the IEEE; Japan Society of Power Electronics; Society of Instrument and Control Engineers; and Japan Society of Mechanical Engineers.

Takamasa Hori graduated in 1961 from the Department of Electrical Engineering, Osaka University, and received his Dr. of Eng. degree later. He joined Hitachi Research Laboratory, Hitachi, Ltd. in 1961. He has been a Professor in the Department of Electrical Engineering, Mie University, since January 1987. He received a Paper Award from the I.E.E., Japan in 1993 and an Achievement Award from the I.E.E., Japan in 1994. He is an IEEE Fellow, and a Fellow of the Society of Instrument and Control Engineers. He also is a member of the Institute of Systems, Control and Information Engineers; and Japan Society of Power Electronics.